ARTICLE

Supporting Information

Preferred coordination of polymer at MOFs enables improved lithium-ion battery anode performance

Muhammad Idrees,[*ab] Saima Batool,[cb] Muhammas Sufyan Javed[e], Muhammad Aizaz Ud Din,[f] Muhammad Imran,[g]

Zhangwei Chen[*ad]

[a]Additive Manufacturing Institute, College of Mechatronics and Control Engineering, Shenzhen University, Shenzhen 518060, PR China

[b]Institute of Microscale Optoelectronics, Shenzhen University, Shenzhen 518060, PR China

[c]Institute for Advanced Study, Shenzhen University, Shenzhen 518060, PR China

[d]Guangdong Key Laboratory of Electromagnetic Control and Intelligent Robotics, College of Mechatronics and Control Engineering, Shenzhen University, Shenzhen, 518060, PR China

[e]School of Physical Science and Technology, Lanzhou University, Lanzhou 730000, PR China

[f]School of Materials and Energy, Southwest University, Chongqing 400715, PR China

[d]Department of Chemistry, Faculty of Science, King Khalid University, P. O. Box 9004, Abha 61413, Saudi Arabia

[*]Corresponding Authors, E-mail: m.idrees8223@gmail.com (M. Idrees); chen@szu.edu.cn (Z. Chen)

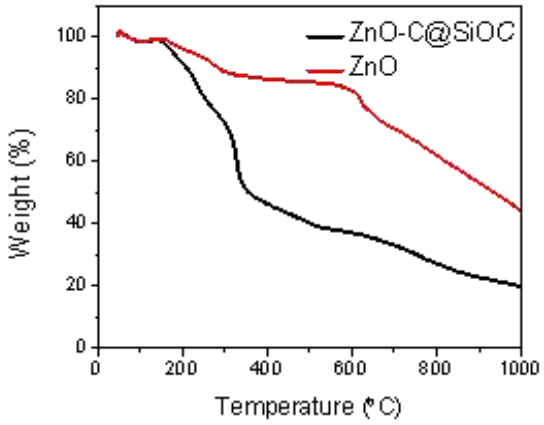

Figure S1. TGA of ZnO and ZnO-C@SiOC nanocomposite.

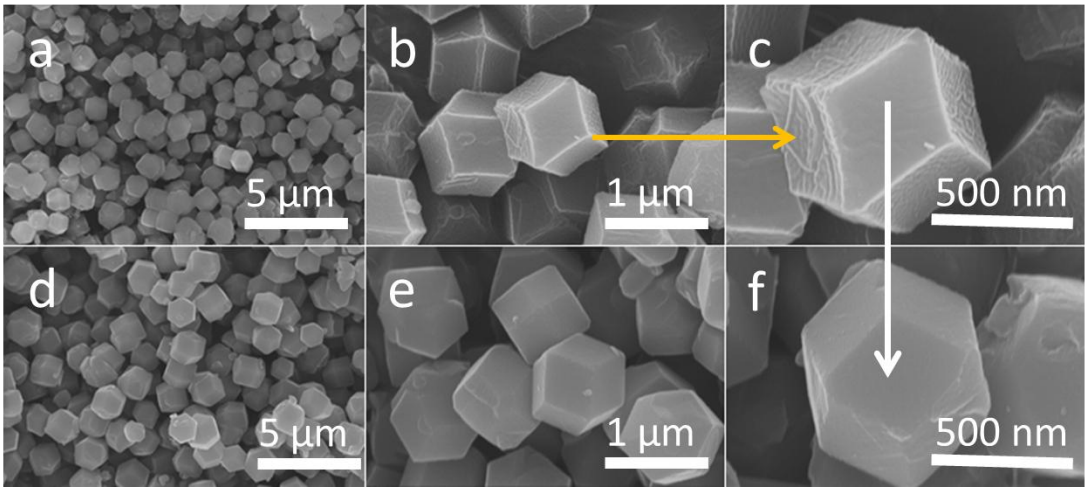

Figure S2. (a-c) SEM and HR-SEM images of ZIF-8 and (d-f) the corresponding pyrolyzed ZnO-C images.

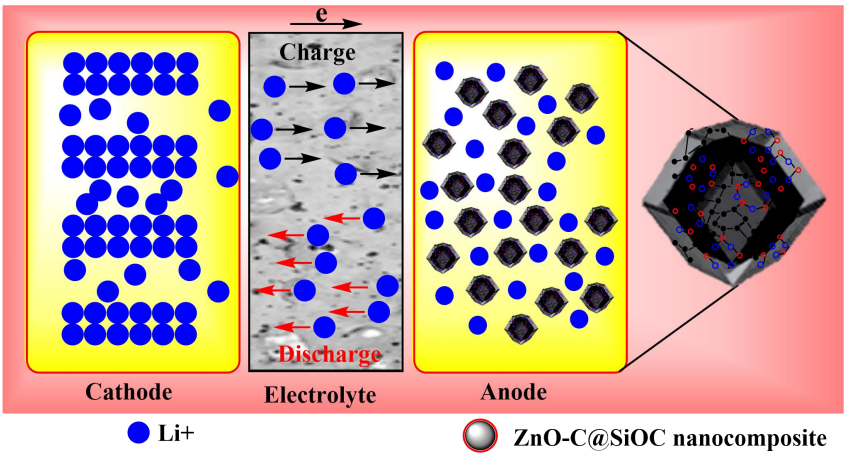

Figure S Charge and discharge phenomenon in ZnO-C@SiOC nanocomposite.

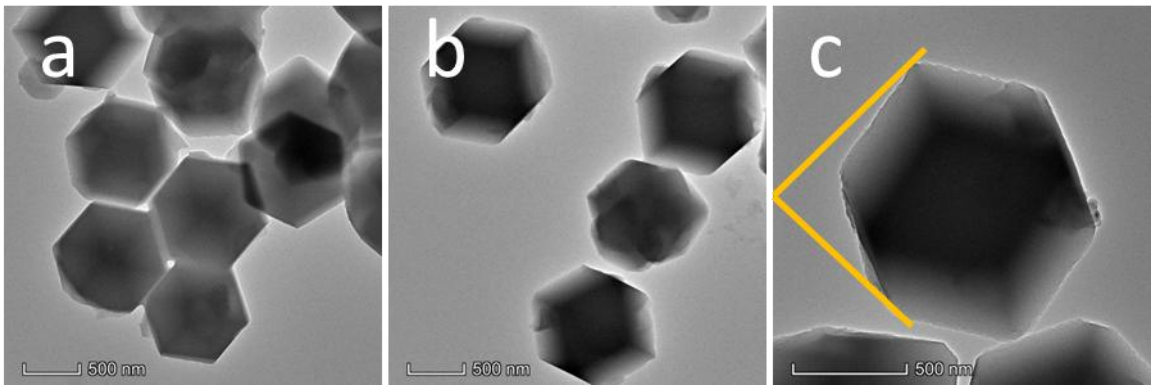

Figure S4. HR-TEM images of pyrolyzed ZIF-8 (ZnO-C) polyhedrons at different magnification.

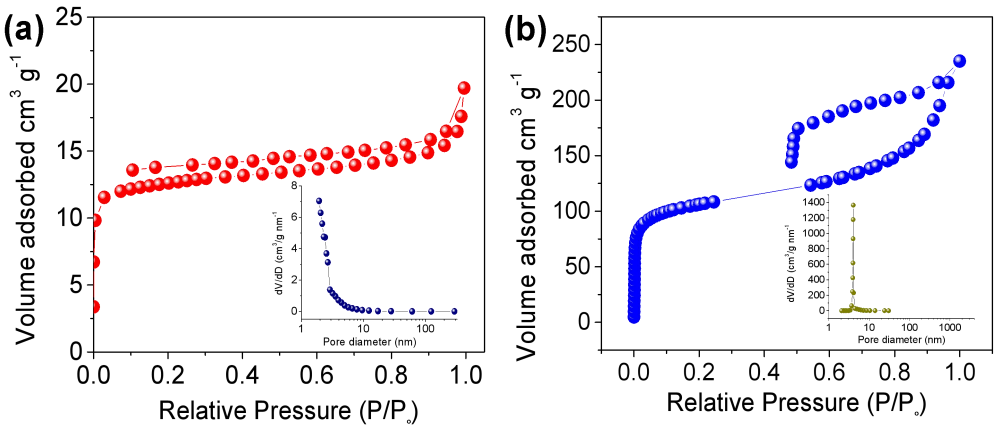

Figure S5. Nitrogen adsorption-desorption isotherms and their corresponding pore size distribution of (a) ZnO-C and (b) ZnO-C@SiOC nanocomposite.

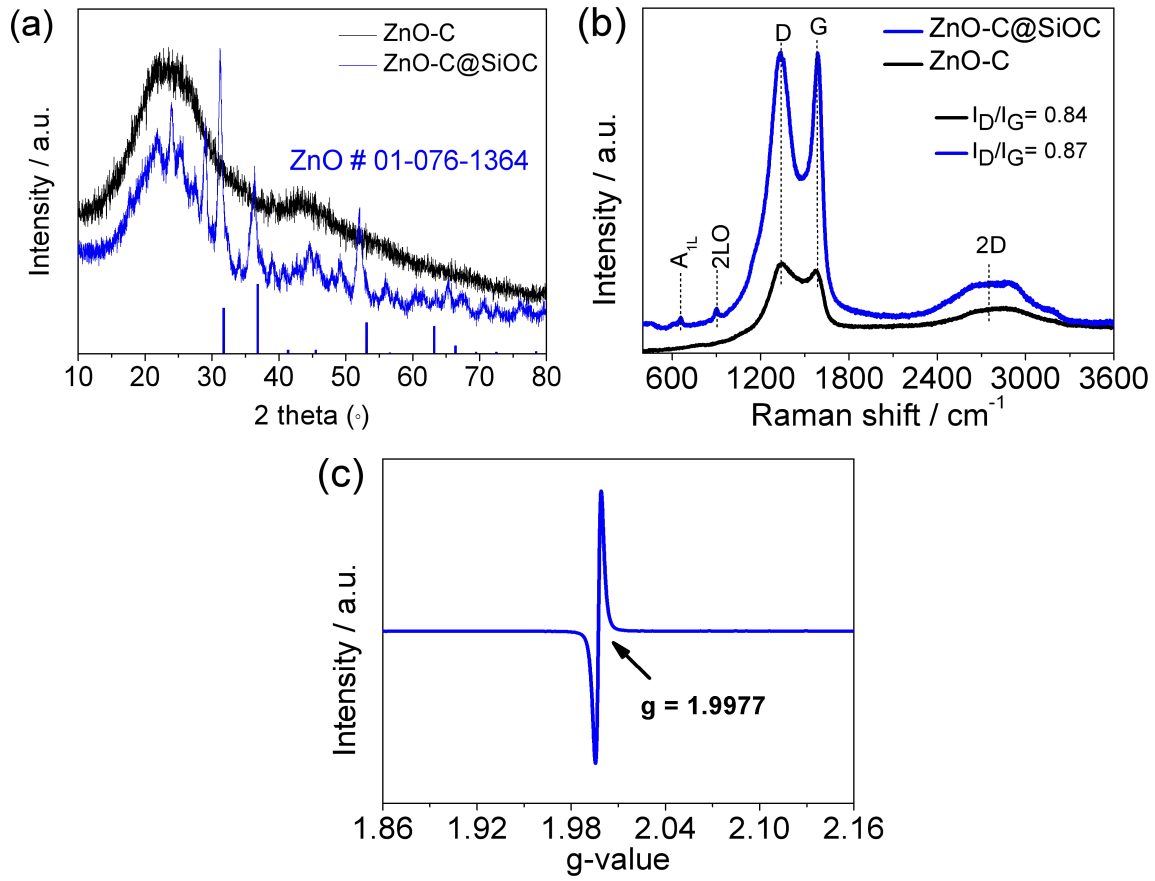

Figure S6. (a) XRD patterns and (b) Raman spectra of ZnO-C and ZnO-C@SiOC nanocomposite. (c) EPR spectra of ZnO-C@SiOC nanocomposite.

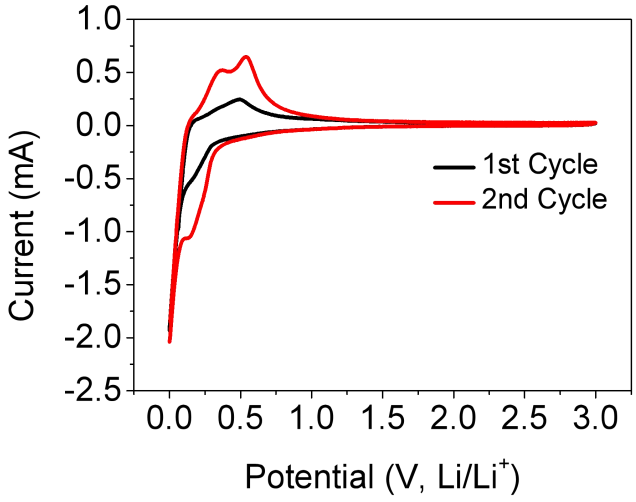

Figure S7. CV curves of ZnO-C anode at 0.02 mV s^{-1}.

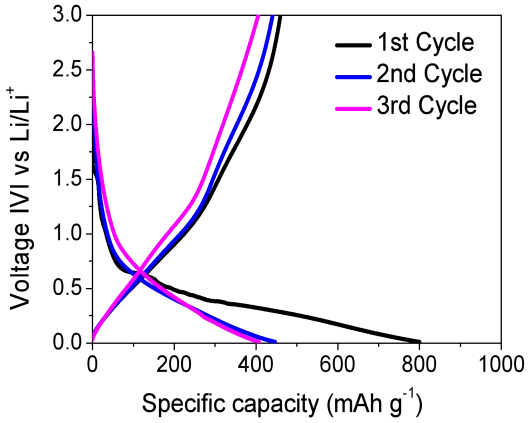

Figure S8. Galvanostatic charge-discharge profiles of the ZnO-C anode at 0.1 A g^{-1}.

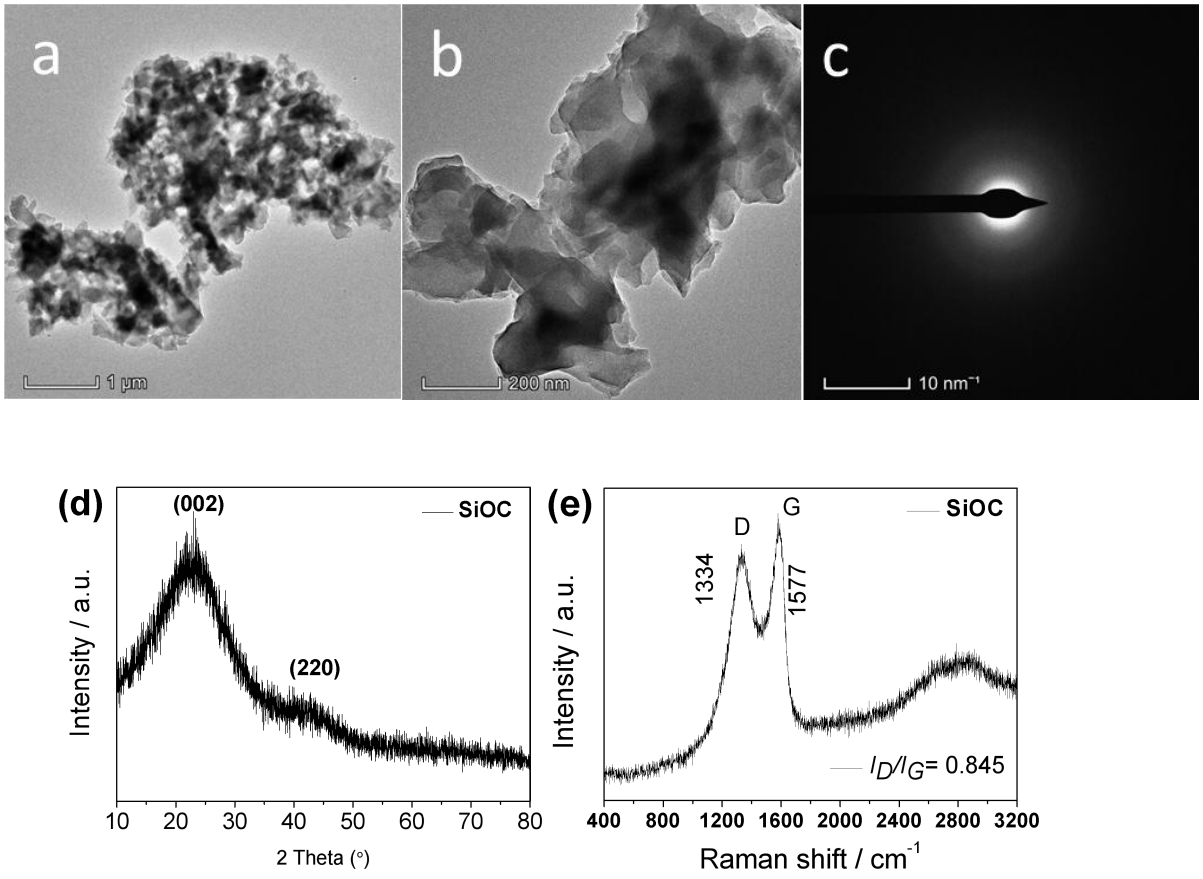

Figure S9. TEM and HR-TEM images (a, b), X-ray diffraction pattern (d) and Raman spectra of SiOC specimen confirming the amorphous nature.

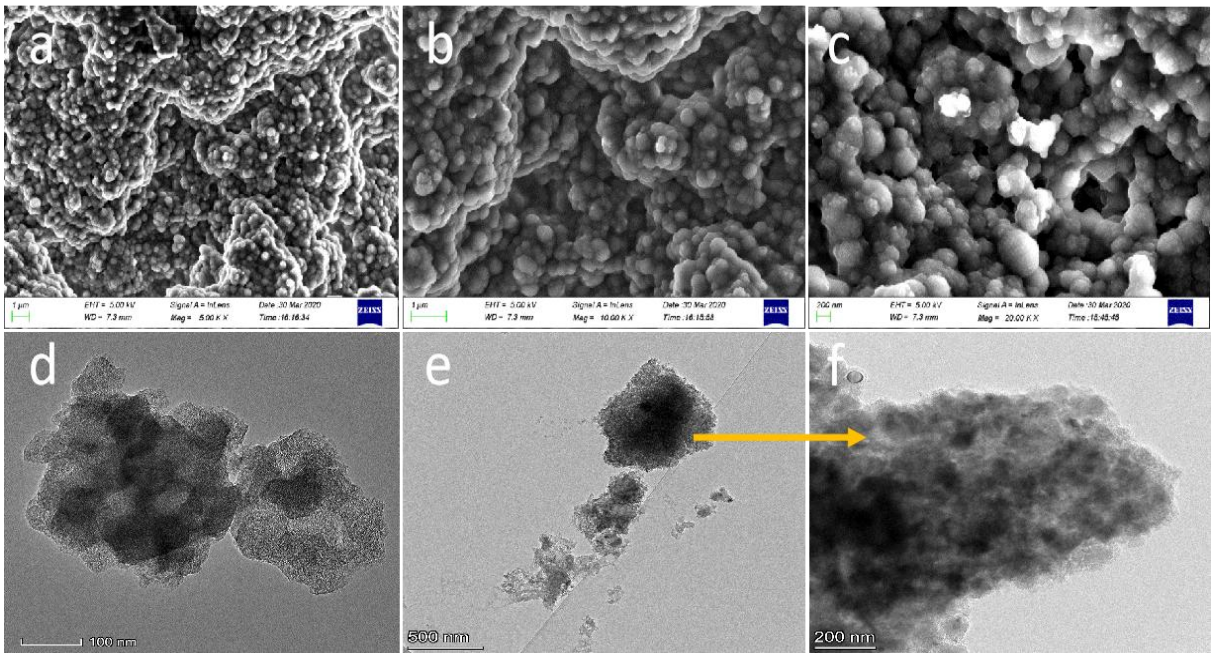

Figure S10. SEM images of cycled ZnO-C@SiOC nanocomposite at (a, b) low and (c) high magnification. HRTEM images of cycled (d) ZnO-C and (e, f) ZnO-C@SiOC nanocomposite anode materials.

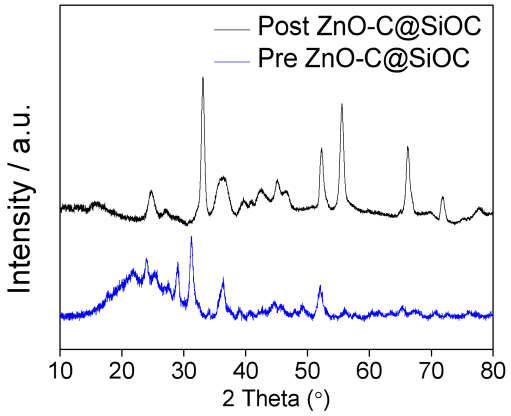

Figure S11. Ex-situ XRD pattern recorded at charge state after 100 cycles for lithium-ion half-cell.

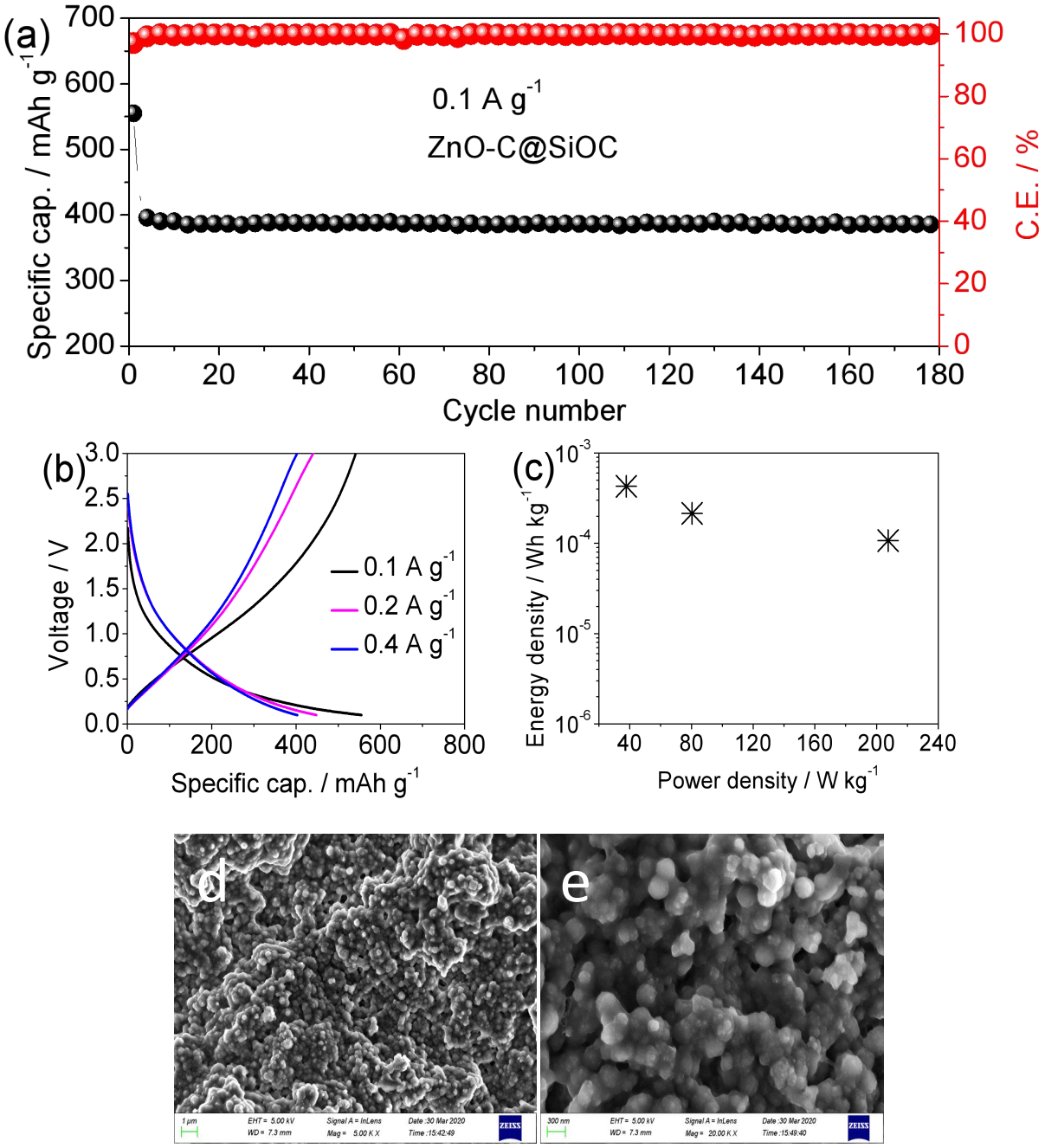

Figure S12. (a) Cycling stability and Coulombic efficiency at 0.1 A g^{-1}, (b) galvanostatic chare-dischareg profiles at different current densities, (c) energy ensity and power densities of ZnO-C@SiOC nanocomposite for lithium-ion full cell and. (c) low and (d) high resolution SEM images of cycled ZnO-C nanocomposite at charge state for lithium-ion full-cell.

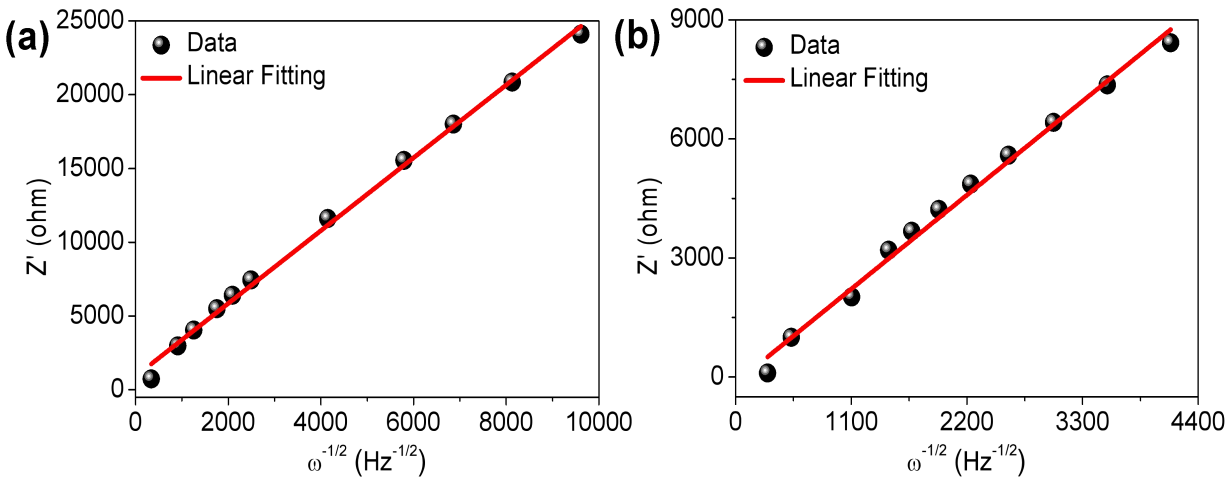

Figure S13. Linear fitting of Z' *vs.* $\omega^{-1/2}$ at low frequency range for (a) ZnO-C and (b) ZnO-C@SiOC nanocomposite anodes.

Table S1. Comparison of the electrochemical performance of ZnO-based anode materials.

Anode material	First discharge/charge capacity (mAh g^{-1})	Specific capacity (mAh g^{-1})	Cycles No. (nth)	Reference
ZnO/carbon black	~1572/1081 at 100 mA g^{-1}	769.5	500	[1]
ZnTe/C	690/530 at 100 mA g^{-1}	623	200	[2]
ZnO/graphene oxide	~1540/780 at 100 mA g^{-1}	752.8	65	[3]
ZnO/multiwalled CNT	1477/845 at 100 mA g^{-1}	419.8	100	[4]
ZnO@ZnO QDs/C Core-shell NRAs	~1610/1160 at 100 mA g^{-1}	699	100	[5]
ZnO nanosheets	1523/~780 at 200 mA g^{-1}	421	100	[6]
Ge-Doped ZnO	1496.5/1014 at 100 mA g^{-1}	~690	100	[7]
Zn_4Sb_3 nanotubes	1160/~590 at 100 mA g^{-1}	450	100	[8]
ZnS/C nanoparticles	1157/694 at 100 mA g^{-1}	506	600	[9]
ZnO-C@SiOC nanocomposite	1364/911 at 100 mA g^{-1}	~940	80	This work
//		~592	500	This work
//		~472	1000	This work

References

1. S. Lu, H. Wang, J. Zhou, X. Wu and W. Qin, Atomic layer deposition of ZnO on carbon black as nanostructured anode materials for high-performance lithium-ion batteries, *Nanoscale*, 2017, **9**, 1184-1192.
2. C. Kim, J. W. Kim, H. Kim, D. H. Kim, C. Choi, Y. S. Jung and J. Park, Graphene oxide assisted synthesis of self-assembled zinc oxide for lithium-ion battery anode, *Chemistry of Materials*, 2016, **28**, 8498-8503.
3. Y. Zou, Z. Qi, Z. Ma, W. Jiang, R. Hu and J. Duan, MOF-derived porous ZnO/MWCNTs nanocomposite as anode materials for lithium-ion batteries, *Journal of Electroanalytical Chemistry*, 2017, **788**, 184-191.
4. L. Wang, G. Zhang, Q. Liu and H. Duan, Recent progress in Zn-based anodes for advanced lithium ion batteries, *Materials Chemistry Frontiers*, 2018, **2**, 1414-1435.
5. G. Zhang, S. Hou, H. Zhang, W. Zeng, F. Yan, C. C. Li and H. Duan, High-performance and ultra-stable lithium-ion batteries based on MOF-derived ZnO@ZnO quantum Dots/C core–shell nanorod arrays on a carbon cloth anode, *Advanced Materials*, 2015, **27**, 2400-2405.
6. Y. Sun, G. Yang, H. Cui, J. Wang and C. Wang, $Zn_xGe_{1-x}O$ 3D micronano structures with excellent performance as anode Material in lithium ion battery, *ACS Applied Materials & Interfaces*, 2015, **7**, 15230-15239.
7. Q. Xie, L. Lin, Y. Ma, D. Zeng, J. Yang, J. Huang, L. Wang and D.-L. Peng, Synthesis of ZnO-Cu-C yolk-shell hybrid microspheres with enhanced electrochemical properties for lithium ion battery anodes, *Electrochimica Acta*, 2017, **226**, 79-88.
8. J. Xu, H. Wu, F. Wang, Y. Xia and G. Zheng, Zn_4Sb_3 nanotubes as lithium ion battery anodes with high capacity and cycling stability, *Advanced Energy Materials*, 2013, **3**, 286-289.
9. X. Du, H. Zhao, Z. Zhang, Y. Lu, C. Gao, Z. Li, Y. Teng, L. Zhao and K. Świerczek, Core-shell structured ZnS-C nanoparticles with enhanced electrochemical properties for high-performance lithium-ion battery anodes, *Electrochimica Acta*, 2017, **225**, 129-136.